## Post-Print

**When citing this work, cite the original published paper.**

**A combined fracture mechanical - rheological study to separate the contributions of hydrogen bonds and disulphide linkages to the healing of poly(urea-urethane) networks**

A. M. Grande*, J. C. Bijleveld, S. J. Garcia, S. van der Zwaag

Novel Aerospace Materials, Faculty of Aerospace Engineering, Delft University of Technology, Kluyverweg 1, 2629 HS, Delft, the Netherlands

*e-mail corresponding author: a.m.grande@tudelft.nl

## Abstract

This work presents a detailed study into the rheological properties and fracture healing behaviour of two poly(urea-urethane) polymers containing (i) hydrogen bonds and (ii) hydrogen bonds and disulphide linkages. The experimental procedure here presented using the temperature and time superposition allowed for the identification of the contribution of each reversible bond type to the network behaviour (rheology) and healing (fracture). During the experimental data analysis it was found that the same shift factors required to construct the rheological master curves from separate isothermal small-amplitude oscillatory shear (SAOS) measurements at different temperatures could also be applied to obtain a master curve for the fracture healing data as a function of healing time and temperature. This work shows therefore the apparent direct relationship between rheological response and macroscopic fracture healing.

# 1. Introduction

In recent times several strategies have been investigated by polymer chemists to design and synthesize new polymeric materials with a so-called intrinsic healing functionality [1-6]. Intrinsic self-healing polymers have the natural ability to make surface scratches disappear and to restore mechanical integrity across a crack when exposed to an appropriate thermal stimulus. The mechanism behind the self-healing is the re-formation of broken (reversible) chemical and/or physical bonds. While spectroscopic and rheological techniques are useful tools to investigate the dynamic and reversible behaviour of healable polymers at the molecular level [7-10], robust techniques capable of quantifying the relevant interfacial healing processes at soft polymer interfaces are less well established [11]. To date, most researchers have used the recovery of tensile strength of broken samples as a measure of interfacial healing. However this testing method fails to capture the relevant chemical processes at the healing interfaces as well as the effective restoration of mechanical integrity. Recently, we presented a fracture mechanics testing procedure based on the application of the J-integral to determine the real state of interfacial healing for a supramolecular elastomer with a higher degree of accuracy than tensile testing [12]. The J-integral method, originally developed to determine the strain energy release rate for crack growth in elasto-plastic materials [13, 14], is nowadays employed to experimentally evaluate the fracture energy of soft materials such as elastomers [15-17], making it also a most appropriate technique for quantification of mechanical properties restoration. In the fracture mechanical method, the structural discontinuity at the interface in its various stages of healing is properly taken into account when measuring the restoration of mechanical integrity as a function of healing time and temperature. The method also allows detecting the transition at the healing crack from a weak interface into a strong interface/interphase. It is then clear that healing in the so far studied intrinsic healing polymers involves both segmental and full molecular motion as well as local re-formation of reversible bonds with different bond energies.

The time and temperature dependence of molecular motions in supramolecular materials, elastomers and polymers is conventionally measured using small-amplitude oscillatory shear (SAOS) rheology and stress relaxation experiments. A full picture of the main relaxation processes exhibited by a polymer over a broad time or frequency domain can be obtained by the application of the time-temperature superposition (TTS) principle, in which the results at different temperatures and time scales are used to form a so-called master curve [18]. In the present work we use the TTS principle on both rheological and fracture mechanical data to demonstrate the correlation between these two tests thereby reinforcing the link between network behaviour and macroscopic healing. The measurements were performed on a poly(urea-urethane) network polymer containing only hydrogen bonds or both hydrogen and dynamic disulphide linkages [19].

## 2. Experimental

### 2.1. Materials

Several experimental analyses, involving amongst others rheology and fracture mechanics testing, were carried out to evaluate the healing capability of elastomers incorporating reversible bonds. The healable material, synthesized based on a procedure as reported in literature [19], consisted of an isocyanate-terminated pre-polymer organized in a network connected by aromatic disulphides linkages and containing urea related H-bonds (here on PUU-SS). A permanently cross-linked polymer network not containing a reversible disulphide linker but keeping the urea H-bonds was also prepared (PUU-CC) to serve as the reference material. FT-IR and Raman spectroscopy were employed to follow the various steps in the polymer synthesis (Supporting Information, Figure S1 and Figure S2). A sketch of the structure of the two polymers is presented in
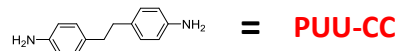
Figure 1.
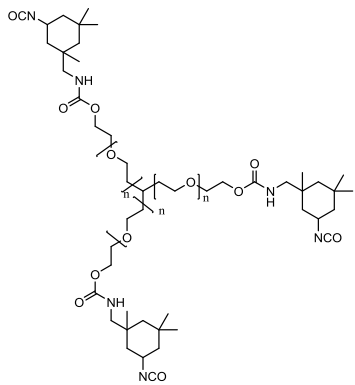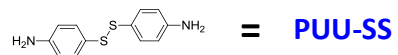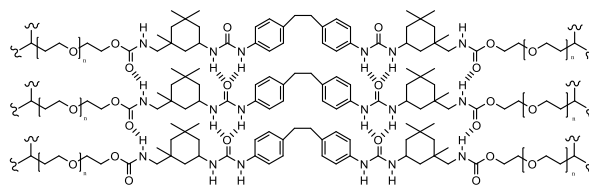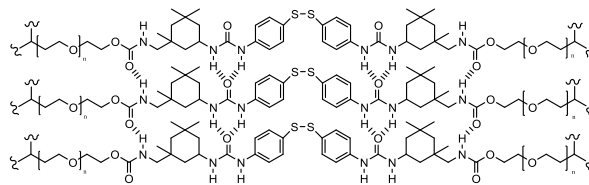
Figure 1: Starting from the same three-arm molecules (pre-polymer), polymer networks with a permeant (PUU-CC) or a dynamic (PUU-SS) linker were synthetized (a). Sketch of the final structure of the two polymers are shown in the lower panel (b).

## 2.2. Testing procedures

Swelling experiments were performed to determine cross-linking density in both polymers. Small samples were cut from the sheets synthesized and swollen for 48 h in tetrahydrofuran (THF). Mass

swelling ratios were obtained by comparing the weight of the different samples before and after the swelling experiments.

Thermal properties of the PUU-SS and PUU-CC material were investigated by means of Differential Scanning Calorimetry (DSC) and thermogravimetric analysis (TGA) over the temperature range from -100 to 100 °C and from 25 to 400 °C, respectively; in both experiments a heating rate of 20 °C/min was employed.

Dynamic and steady-state rheological measurements were performed on a Thermo Scientific (model Haake™ Mars III) rheometer equipped with a temperature controlled test chamber. A 20 mm parallel plate geometry was employed for all the measurements. For the dynamic rheological tests, temperature sweep experiments at a frequency of 1 Hz were performed in the linear viscoelastic regime (0.5% strain). A heating rate of 5 °C/min from -30 to 180 °C was employed. Frequency sweep experiments (0.01-10 Hz) were also carried out in the small amplitude range (0.5% strain) at various temperatures. In order to construct rheological master curves, 20 °C temperature increments were adopted in the domain 20 to 180 °C. Steady-state relaxation experiments at a constant temperature of 120 °C were performed by applying a deformation step of 0.5% strain and recording the shear stress evolution for at least $10^4$ s.

Single Edge Notch Tensile (SENT) fracture experiments were performed using a Zwick mechanical testing machine (model 1455) fitted with a 2 kN load cell. Rectangular samples (70x20 mm) were cut with a die from the moulded 2 mm flat polymeric sheets. A cut with a length of 10 mm was made into the centre of the longest side of each specimen using a sharp razor and the notch tip was immediately sprinkled with talcum powder in order to avoid contact between the freshly cut surfaces. Pre-notched samples were then clamped in the tensile machine with a gauge length of 40 mm and stretched until failure. Subsequently, fractured samples were accurately positioned in PTFE moulds and healed according to a previous published procedure [12]. The effects of both healing time and healing temperature on the recovery of fracture properties were investigated. Different samples were healed at various constant temperature for 1, 3, 6 or 24 h; the healing

temperature ranged from room temperature (RT≈20 °C) to 120 °C. In the case of healing above RT, heated samples were exposed to and equilibrated at RT for 30 min before being re-tested following the same SENT fracture protocol. Samples healed at RT were retested right after the healing treatment. A constant cross-head separation velocity of 1 mm s$^{-1}$ (initial strain rate $\dot{\varepsilon}$ = 2.5·10$^{-2}$ s$^{-1}$) was employed in each experiment and force and displacement data were collected. All the fracture tests were performed at room temperature. The typical duration of a fracture mechanics test was less than 40 s. At least three samples were used for each testing conditions. Video images were recorded during each experiment in order to detect crack initiation and to follow crack evolution as shown in Figure 2. In the video footage the different fracture behaviour at the healed crack can be observed highlighting the interface-interphase transition in the PUU-SS sample.



Figure 2: Representative video frames recorded during fracture experiments for virgin and healed (1 hour at RT and 1 hour at 120 °C) on the PUU-SS system. Testing times marked with asterisk (*) indicate the crack initiation.

# 3. Results

## 3.1. Fracture and healing measurements

Figure 3 shows representative Load-Displacement curves for virgin and (1 hour) healed PUU-SS and PUU-CC samples. The PUU-SS material shows a clear temperature dependent recovery of the mechanical response with an increasing degree of healing with increasing healing temperature. The initial modulus value is quickly restored, but the load displacement curves consistently fall below the curve for the virgin material at higher strain levels. In contrast the PUU-CC system presents a limited recovery of the initial properties even after healing for 1 hour at the highest temperature (120 °C).
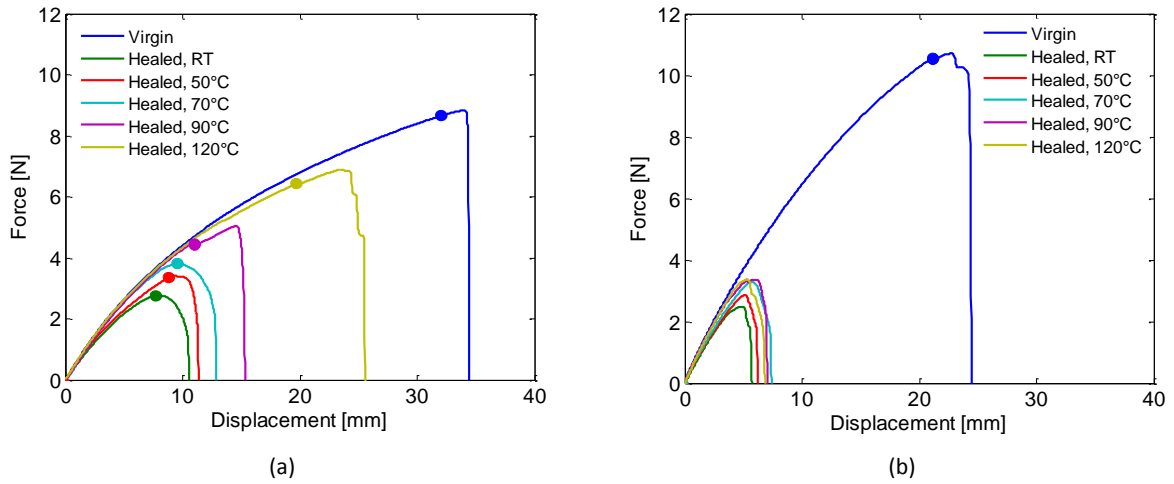


Figure 3: Load-Displacement curves for virgin and (1 hour) healed PUU-SS (a) and PUU-CC (b). Crack initiation points for different samples are highlighted; for PUU-CC healed samples crack initiation points were omitted for clarity.

From these Load-Displacement curves, fracture properties can be determined using the J-integral analysis method [12, 16]. Critical fracture energy values, $J_c$, for each sample were calculated according to the following equation:

$$J_c \ [\text{kJ/m}^2] = \left. \frac{\eta U_c}{b(w-a)} \right|_{u_c} \tag{1}$$

where $U_c$ is the energy calculated as the area under the Load-Displacement curves at the displacement $u_c$ where crack propagation occurs as selected from the video recordings and J-integral approach, $\eta$ is the proportionality factor related to sample geometry (a value of 0.9 was selected according to literature [16]); $b$, $w$ and $a$ are the sample thickness, sample width and pre-crack length, respectively.

It is worth noting that virgin PUU-SS showed a greater $J_c$ value than virgin PUU-CC (see Supporting Information, Table S5) indicating that during fracture testing more energy is dissipated for the sulphur containing polymer. This may be related to the different kind of linkage (dynamic covalent versus permanent covalent for PUU-SS and PUU-CC, respectively) forming the two polymer networks [20]. The dynamic nature of the polysulphide bonds may thus introduce an additional dissipative process not available in the same polymer only containing one kind of reversible bonds (PUU-CC) [21].

At healing temperatures above 70 °C the fracture toughness values of the PUU-SS material clearly increased with healing time and temperature (Table S5). No such increase with contact time was observed for RT and 50 °C healing cycles. In case of the PUU-CC material the healed samples exhibited nearly equal low fracture energies regardless of the healing time and healing temperature.

The calculated $J_c$ values were then used to obtain a more quantitative analysis of the healing capability defining healing efficiency as the quotient of the fracture energy after healing ($J_c^{healed}$) and the fracture energy of the pristine material ($J_c^{pristine}$):

$$Healing\ efficiency\ [\%] = \frac{J_c^{healed}}{J_c^{pristine}} \cdot 100 \qquad (2)$$

The healing efficiency values for PUU-SS and PUU-CC are plotted in Figure 4.a and 4.b, respectively. As expected, for the disulphide containing system a high temperature and a longer healing time significantly increased the healing efficiency resulting in a maximum fracture energy recovery of

about 55% after a 6 h healing treatment at 120 °C. The reference polymer, PUU-CC, shows on the other hand a maximum healing efficiency of only 10% after the same high temperature healing treatment. At RT and 50 °C, the same low healing efficiency for both PUU-CC and PUU-SS systems is calculated.
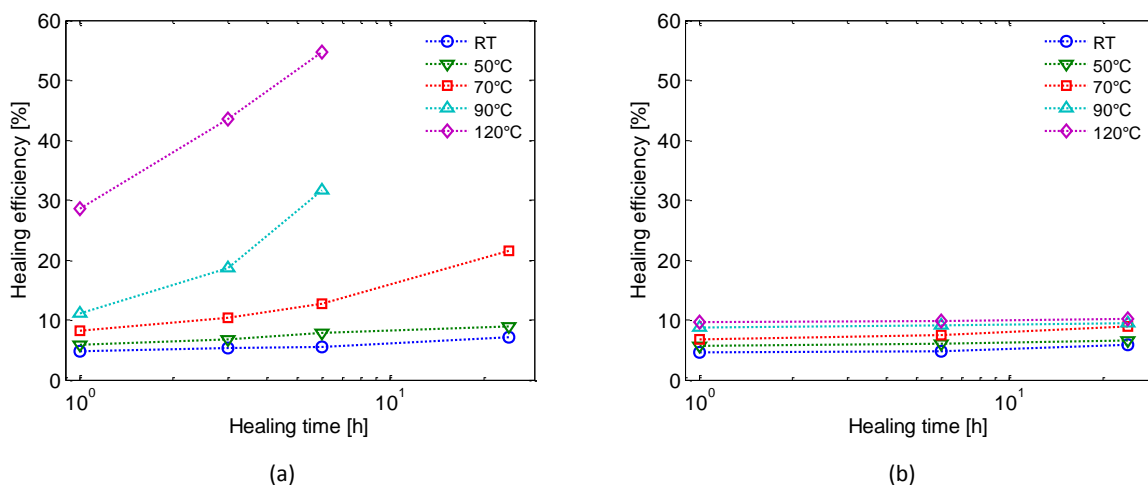


Figure 4: Healing efficiency from fracture experiments for PUU-SS (a) and PUU-CC (b) samples healed for different time and at different temperature.

## 3.2. Rheological measuraments

In figure 5 the results of the rheological measurements as a function of temperature are shown for both polymer systems. Both the shear storage moduli ($G'$) and shear loss moduli ($G''$) present a similar temperature dependence under these testing conditions with a predominance of the elastic component ($G' > G''$) over the entire temperature range. In the low temperature regime (< 0 °C), $G'$ and $G''$ values are comparable for both polymers. Small variations in the mechanical response can be attributed to slightly different glass transition temperatures (Figure S3, DSC measurements). At high temperatures (> 100 °C), both polymers seem to reach a rubbery plateau in the 0.1-0.2 MPa $G'$ range although a lower plateau is observed for PUU-SS, probably indicating a lower cross-linking density. This result was confirmed by the room-temperature swelling experiments in THF yielding mass swelling ratios of 7.0 and 5.6 for PUU-SS and PUU-CC, respectively. In the intermediate temperature

range (0-100 °C), the broad tan(δ) peak exhibited by both polymers indicates the occurrence of a specific relaxation process. Some clear differences in the position and extension of this peak are detectable, with the PUU-CC material showing the damping peak at lower temperature. A possible explanation of the origin of such differences can be related to the mobility of the three-arm molecules during the polymer production step. While in PUU-CC the connect molecules are "locked" after curing, in PUU-SS, the three-arm molecules still have sufficient mobility due to temperature triggered disulphide reshuffling under (high temperature) processing conditions [22]. This latter mechanism can potentially allow a reorganization of the network structure thus affecting the final mechanical response of the sulphur containing polymer [23]. However, extensive studies on the gelation kinetics of the two polymers are required to resolve this issue and fall out of the scope of the current work.
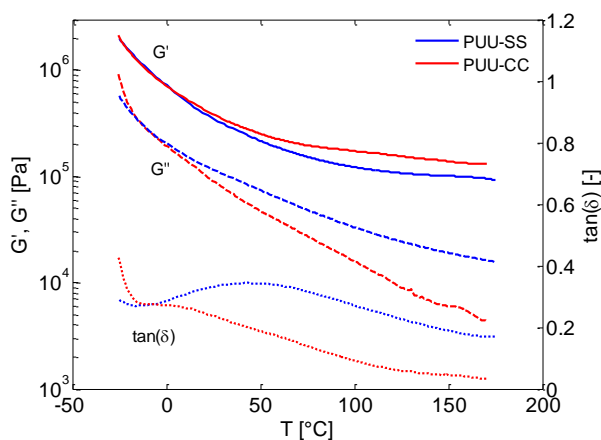


Figure 5: Temperature sweeps for PUU-SS and PUU-CC.

The results of the stress-relaxation tests at a constant temperature of 120 °C (which is well below the degradation temperature, Figure S4) are presented in Figure 6. The two materials exhibit a clearly different relaxation response. As expected, the permanently bonded polymer (PUU-CC) showed an almost steady shear modulus ($G$) over a wide relaxation time range; only at longer times a relaxation is detectable, which can be due to the cleavage of urethane/urea groups [24, 25]. Since its time scale

is much longer than those time scales studied in this work the potential effect of its reversibility nature on the network reorganization during healing is here neglected. On the other hand, PUU-SS exhibited a prominent decrease in the shear modulus after about $10^3$ s indicating that, under these experimental conditions, this polymer behaves more like a viscoelastic liquid than a viscoelastic solid.
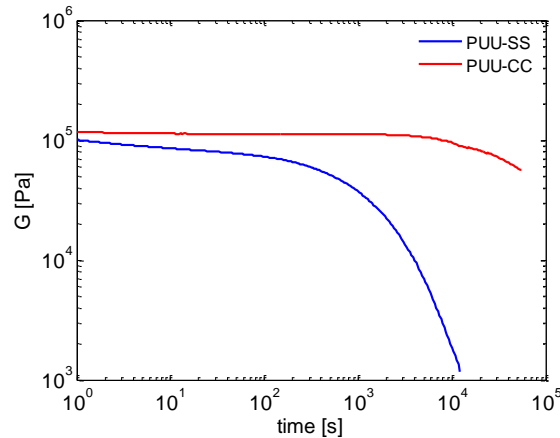


Figure 6: Relaxation tests at 120 °C (b) for PUU-SS and PUU-CC.

Frequency sweep measurements at different temperatures (Figure 7) confirm the hypotheses based on the previous experimental data. At low temperature (20 °C), the two polymers show a similar mechanical response following shear oscillation in the liner viscoelastic regime; the storage modulus dominates in all the frequency range and the systems exhibit elastic behaviour. A divergence appears with increasing temperature where the loss modulus becomes more significant for PUU-SS (Figure 7.a). The predominance of the viscous response ($G'' > G'$) becomes clear for the disulphide based system at 180 °C. This high temperature relaxation process can be related to the breaking/reforming rate of reversible bonds embedded in the polymer [23, 26-28]. The inverse frequency of $G'$- $G''$ intersection is usually associated to the characteristic relaxation time of the transient polymeric network [29].
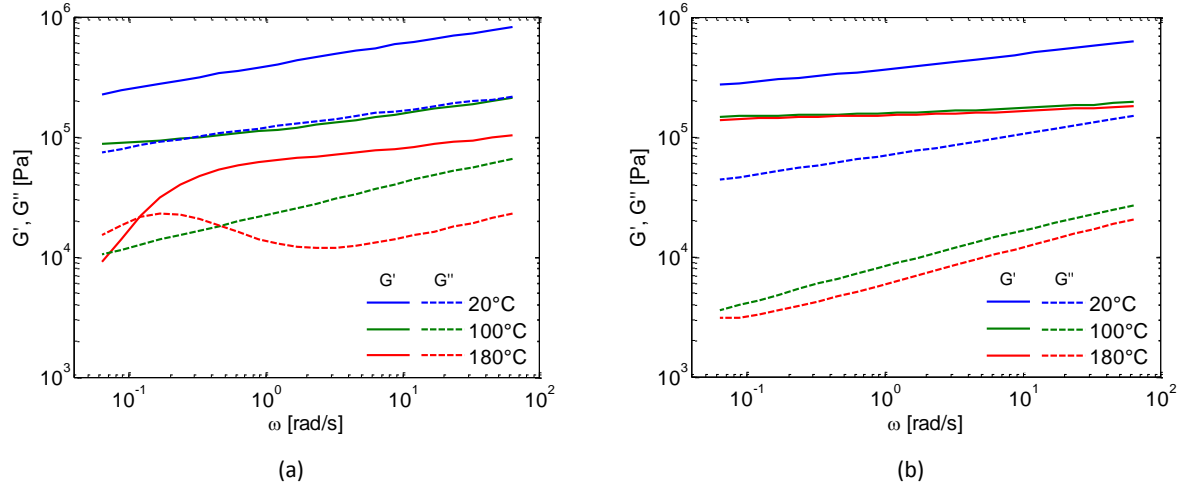
Figure 7: Frequency sweeps at different temperature for PUU-SS (a) and PUU-CC (b).

## 4. Discussion

### 4.1. Fracture strength of the healed interface

The recovery of fracture strength of the PUU-CC and the PUU-SS material showed both similarities and differences. At low temperatures  (RT and 50 °C) both polymers show a marginal recovery of the fracture strength, which was obtained within the first hour of healing and did not increase when the healing time was increased to 24 hours. For the PUU-CC material the same level of marginal recovery was obtained when the healing temperature was raised up to 120 °C. In contrast, the PUU-SS material showed a marked increase in healing efficiency with time and temperature for 70 °C and beyond. Given the chemical compositions of the two polymers it is most likely that the healing efficiency of the PUU-CC material is due primarily to the H-bonds between the urea groups [19] which are the reversible moieties with the strongest bond energy present in this polymer. The H-bond re-formation is fast and the spatial distribution of these bonds along the polymer backbone is rather high. Hence the recovering in fracture toughness reaches its maximum level rather quickly and shows no real time dependence. By analogy it is likely that the low temperature (RT and 50 °C) healing in the PUU-SS material is also due to the reversible H-bonds. In contrast, the clear and marked increase in fracture toughness in the PUU-SS material must then be due to the dynamics of

the disulphide bonds [10, 23, 27, 30-32]. Given the lower density of disulphide bonds and their intrinsic slower kinetics a stronger time dependence of the healing efficiency is to be expected in the explored healing time frame.

## 4.2. Time-Temperature dependence of rheological and healing properties

In linear viscoelastic rheology, the time-temperature superposition principle allows estimating the dynamics of polymeric systems over very broad timescales. Its rigorous application implies that the microstructure of the material is independent on temperature, that relaxation processes show the same temperature-dependence and that there are no chemical changes due to temperature [18]. These conditions are not always valid for thermo-rheological complex materials such as polymers with transient networks based on non-covalent or dynamic covalent bonds [33, 34]. However, TTS can still be a useful tool to investigate the time-dependent relaxation processes for these non-conventional polymers [35-39].

Figure 8 depicts master curves of $G'$ and $G''$ (reference temperature of 20 °C) for PUU-SS after application of an appropriate time-temperature superposition procedure. Details on the construction of rheological master curves are presented in the Supporting Information (Figure S6). The material response can be divided into two regimes in relation to the terminal relaxation ($\tau_d$): (i) a narrow regime for $t > \tau_d$ ($\tau_d = 1/\omega_d$, where $\omega_d$ is the $G'$- $G''$ crossover frequency) associated with the terminal relaxation and (ii) an intermediate-time regime $t < \tau_d$, where a broad relaxation process covering several time/frequency decades is present. A third relaxation process in the short-time regime (high frequencies), related to the polymer glass transition, can be assumed; however this transition, albeit necessary for the network mobility, has a limited effect on the long term relaxations [26].
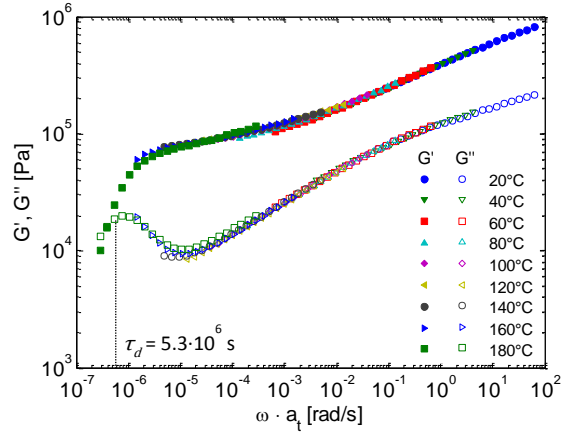
Figure 8: $G'$ and $G''$ master curves for PUU-SS at the reference temperature of 20 °C.

The two separated healing steps observed in healing measurements for PUU-SS can be potentially related to the relevant relaxations located by the TTS analysis at the intermediate and low frequencies ranges. The first healing stage, detected at lower healing temperatures, yielded to a limited recovery of fracture properties due to the re-formation of weak intermolecular reversible H-bonds. This process can be linked to the broad relaxation at intermediate frequency ranges determined by rheological measurements. In the second healing stage, the enhanced interfacial properties recovery after high temperature healing treatments can be associated to the rearrangement of the reversible intramolecular dynamic covalent bonds (disulphide bonds) at the healed interface. This healing process is consistent with the second slower relaxation characterised by a significant decay of the elastic properties and a fluid-like behaviour (high mobility) of the PUU-SS polymer network. This slower relaxation was not observed for PUU-CC (Figure S7).

To further investigate the connection between viscoelastic and healing properties, the time-temperature dependence of the recovery of fracture energy was also studied following the TTS principle. Interestingly, using the well-established procedure for shifting rheological data to form a single master curve, it was possible to build a single fracture toughness healing master curve by shifting along the x-axis the healing efficiency values (Figure 9). Also in this case two regions can be distinguished: for short times a nearly constant low healing efficiency can be observed, followed by

an increase in the healing efficiency for long healing times. In order to analytically describe this healing behaviour some considerations and simplifications can be adopted. As in other disulphide containing polymers [10, 23, 27, 31, 32], the temperature dependent disulphide bond reshuffling can be assumed as the most significant process influencing interfacial recovery as it allows for long term chain movements (terminal relaxation). Additionally, time does not lead to an improvement of the interfacial restoration only due to H-bonding as seen for the PUU-CC sample. The effect of such bonds can thus be considered time independent and with a minor impact on mechanical restoration. Based on these considerations, a simple two-step healing model based on a short term healing component and on a single relevant time-dependent healing process [40] can be selected and adapted to describe the healing efficiency evolution of the PUU-SS system over a broad time range:

$$Healing\ efficiency\ [\%] = HE_0 + HE_a(1 - e^{-t/\tau_h}) \tag{3}$$

where $HE_0$ is the healing efficiency for the short healing time mainly influenced by the H-bonds, $HE_a$ is the contribution to healing of the dominant healing process (disulphide bond exchange for PUU-SS), $\tau_h$ the characteristic time constant of the main healing process and $t$ the healing time. As can be observed in Figure 9, the simple selected equation fits the experimental data with a good accuracy providing indirect support to the aforementioned assumptions.
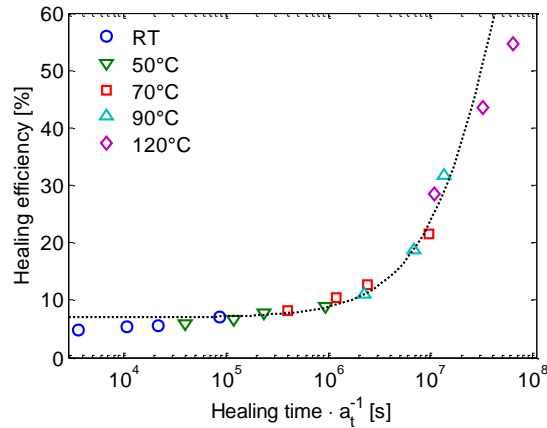
Figure 9: Healing efficiency master curve ($T_{ref}$ = 20 °C) obtained from fracture tests fitted with Equation 3 ($HE_0$ = 7, $HE_a$ = 93 and $\tau_h$ = 5·$10^7$ s)

Interestingly, when plotting the shift factors ($a_t$) derived from the SAOS and fracture healing experiments against the inverse temperature, the data show a remarkably good overlap as shown in Figure 10. While to the best of our knowledge this is the first time that the similarity between shifting rheological data and fracture toughness healing data is demonstrated for a synthetic polymer, recently a similar analysis of the time-temperature dependence of healing efficiency (measured as the recovery of tensile properties) was presented for the generation of the healing master curve of a biological system with a healing mechanism governed by protein-metal bond exchange [41] further highlighting the relationship between synthetic and natural healing systems.
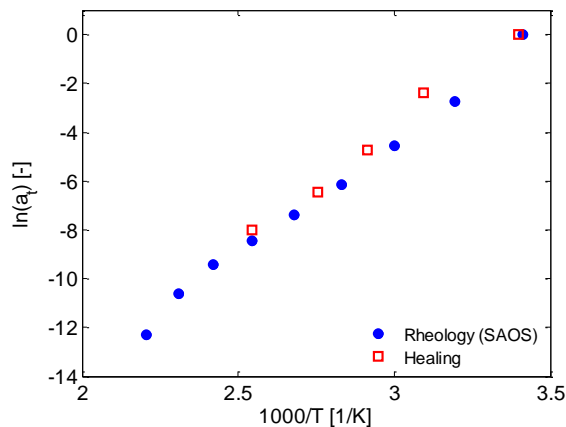


Figure 10: Shift factor ($a_t$) arising from rheological and healing master curves construction for PUU-SS, ($T_{ref}$ = 20 °C).

Based on these findings, it is possible to correlate the effect of the different relaxation processes on the healing performances of PUU-SS. The healing process at short times (related to the broad relaxation determined by rheological measurements) has a limited impact on the fracture resistance of the healed crack. These results indicate that the dynamics of the studied healable polymer (PUU-SS) are mainly dominated by the reshuffling of disulphide bonds (at elevated temperatures) and that the reversible physical bonds (H-bonds) play a secondary role in the healing process. While H-bonds contribute only to the initial sticking or interfacial adhesion, the disulphide linkages and chain interdiffusion contribute to the time-dependent formation of a new interphase at the damaged plane showing high level of mechanical properties restoration and similarity to the original polymer behaviour.

Finally, when looking in detail to the values of the relevant time constants it seems that the characteristic time scale for the healing ($\tau_h$= 5·10$^7$ s) is slightly longer than that for the rheological relaxation ($\tau_d$= 5.3·10$^6$ s). This difference, also observed in other healable systems [40, 42, 43], may be related to the difference in the imposed strains during testing. While in SAOS measurements the polymer network is only weakly deformed, the fracture experiments involve large strain deformation and the generation of fracture surface. Hence, the recovery of reversible bonds across the highly deformed fracture interface may take longer than in a weakly deformed network of higher structural perfection as occurs in the rheology tests [44]. Furthermore, a delay in the healing process due to wetting of the fracture surface may also take place [45]. Notwithstanding the modest difference in absolute time scale constant values, the correspondence of the shift factors in Figure 10 is taken as clear evidence that the same mechanisms determine both the fracture healing and the rheological relaxation phenomena.

## Conclusions

The evaluation of the recovered mechanical properties after damage in healable polymers is a crucial aspect for the implementation of such materials in engineering applications. In this research an advanced experimental procedure based on fracture and rheological measurements was developed in order to gain a deeper understanding of the role of different reversible groups on the macroscopic healing of polymers.

The proposed experimental approach was applied to a self-healing polymer containing reversible chemical disulphide and physical hydrogen bonds and its "not healable" version containing only the reversible physical bonds. The obtained fracture/healing and rheological time-temperature data were analysed according to TTS principle allowing to investigate the healing and viscoelastic responses of the healable material over a broad time/frequency range. A critical insight into the dynamics and the healing potential of the studied system was achieved. In particular, the role on the interfacial strength recovery of each reversible moiety and associated relaxation process was identified and clarified. The temperature-activated healing mechanism allowed for the re-formation of strong covalent bonds at the healing zone leading to the formation of an interphase with similar mechanical behaviour as the pristine material but lower mechanical strength even after longer healing times. This peculiar behaviour was not observed for the reference material, where reversible weak bonds present in the material only provide a limited recovery of the original fracture properties. Furthermore it was found that the dependence of healing efficiency on healing temperature and time was in agreement with the one exhibited by the polymer in SAOS measurements highlighting the existing relation between macroscopic healing and viscoelastic properties. The results also further confirm the previous results reported by the authors with other intrinsic healing polymers indicating that a true 100% restoration of the mechanical properties at the crack plane is not possible with current approaches despite significantly high levels of healing can be achieved.

## Acknowledgments

## References

1. Hager MD, Greil P, Leyens C, Van Der Zwaag S, and Schubert US. Advanced Materials 2010;22(47):5424-5430.
2. Herbst F, Döhler D, Michael P, and Binder WH. Macromolecular Rapid Communications 2013;34(3):203-220.
3. Sandmann B, Bode S, Hager M, and Schubert U. Metallopolymers as an Emerging Class of Self-Healing Materials. In: Percec V, editor. Hierarchical Macromolecular Structures: 60 Years after the Staudinger Nobel Prize II, vol. 262: Springer International Publishing, 2013. pp. 239-257.
4. de Espinosa LM, Fiore GL, Weder C, Johan Foster E, and Simon YC. Progress in Polymer Science 2015;49–50:60-78.
5. Scheiner M, Dickens TJ, and Okoli O. Polymer 2016;83:260-282.
6. Zhang P and Li G. Progress in Polymer Science 2016.
7. Serpe MJ and Craig SL. Langmuir 2007;23(4):1626-1634.
8. Kumpfer JR, Wie JJ, Swanson JP, Beyer FL, Mackay ME, and Rowan SJ. Macromolecules 2012;45(1):473-480.
9. Zedler L, Hager MD, Schubert US, Harrington MJ, Schmitt M, Popp J, and Dietzek B. Materials Today 2014;17(2):57-69.
10. AbdolahZadeh M, C. Esteves AC, van der Zwaag S, and Garcia SJ. Journal of Polymer Science Part A: Polymer Chemistry 2014;52(14):1953-1961.
11. Bode S, Enke M, Hernandez M, Bose R, Grande A, van der Zwaag S, Schubert U, Garcia S, and Hager M. Characterization of Self-Healing Polymers: From Macroscopic Healing Tests to the Molecular Mechanism. Advances in Polymer Science: Springer Berlin Heidelberg, 2015. pp. 1-30.
12. Grande AM, Garcia SJ, and van der Zwaag S. Polymer 2015;56(0):435-442.
13. Rice JR. Journal of Applied Mechanics 1968;35(2):379-386.
14. Cherepanov GP. Journal of Applied Mathematics and Mechanics 1967;31(3):503-512.
15. Hocine NA and Abdelaziz MN. International Journal of Fracture 2003;124(1-2):79-92.
16. Ramorino G, Agnelli S, De Santis R, and Riccò T. Engineering Fracture Mechanics 2010;77(10):1527-1536.
17. Agnelli S, Ramorino G, Passera S, Karger-Kocsis J, and Riccò T. Express Polymer Letters 2012;6(7):581-587.
18. Ferry JD. Viscoelastic properties of polymers: Wiley, 1961.
19. Rekondo A, Martin R, Ruiz de Luzuriaga A, Cabanero G, Grande HJ, and Odriozola I. Materials Horizons 2014;1(2):237-240.
20. Mayumi K, Guo J, Narita T, Hui CY, and Creton C. Extreme Mechanics Letters 2016;6:52-59.
21. Bang E-K, Lista M, Sforazzini G, Sakai N, and Matile S. Chemical Science 2012;3(6):1752-1763.
22. Martin R, Rekondo A, Ruiz De Luzuriaga A, Cabañero G, Grande HJ, and Odriozola I. Journal of Materials Chemistry A 2014;2(16):5710-5715.

23. Canadell J, Goossens H, and Klumperman B. *Macromolecules* 2011;44(8):2536-2541.

24. Delebecq E, Pascault J-P, Boutevin B, and Ganachaud F. *Chemical Reviews* 2013;113(1):80-118.

25. Offenbach JA and Tobolsky AV. *Journal of Colloid Science* 1956;11(1):39-47.

26. Knoben W, Besseling NAM, Bouteiller L, and Cohen Stuart MA. *Physical Chemistry Chemical Physics* 2005;7(11):2390-2398.

27. Yoon JA, Kamada J, Koynov K, Mohin J, Nicolaÿ R, Zhang Y, Balazs AC, Kowalewski T, and Matyjaszewski K. *Macromolecules* 2012;45(1):142-149.

28. Obadia MM, Mudraboyina BP, Serghei A, Montarnal D, and Drockenmuller E. *Journal of the American Chemical Society* 2015;137(18):6078-6083.

29. Rossow T, Habicht A, and Seiffert S. *Macromolecules* 2014;47(18):6473-6482.

30. Owen GDT, MacKnight WJ, and Tobolsky AV. *The Journal of Physical Chemistry* 1964;68(4):784-786.

31. Kamada J, Koynov K, Corten C, Juhari A, Yoon JA, Urban MW, Balazs AC, and Matyjaszewski K. *Macromolecules* 2010;43(9):4133-4139.

32. Lafont U, Van Zeijl H, and Van Der Zwaag S. *ACS Applied Materials and Interfaces* 2012;4(11):6280-6288.

33. Seiffert S and Sprakel J. *Chemical Society Reviews* 2012;41(2):909-930.

34. Kloxin CJ, Scott TF, Adzima BJ, and Bowman CN. *Macromolecules* 2010;43(6):2643-2653.

35. Müller M, Seidel U, and Stadler R. *Polymer* 1995;36(16):3143-3150.

36. Stadler FJ, Pyckhout-Hintzen W, Schumers J-M, Fustin C-A, Gohy J-F, and Bailly C. *Macromolecules* 2009;42(16):6181-6192.

37. Feldman KE, Kade MJ, Meijer EW, Hawker CJ, and Kramer EJ. *Macromolecules* 2009;42(22):9072-9081.

38. Hayashi M, Noro A, and Matsushita Y. *Journal of Polymer Science Part B: Polymer Physics* 2014;52(11):755-764.

39. Callies X, Fonteneau C, Véchambre C, Pensec S, Chenal JM, Chazeau L, Bouteiller L, Ducouret G, and Creton C. *Polymer* 2015;69:233-240.

40. Sheridan RJ and Bowman CN. *Polymer Chemistry* 2013;4(18):4974-4979.

41. Schmitt CNZ, Politi Y, Reinecke A, and Harrington MJ. *Biomacromolecules* 2015;16(9):2852-2861.

42. Thornell TL, Helfrecht BA, Mullen SA, Bawiskar A, and Erk KA. *ACS Macro Letters* 2014;3(10):1069-1073.

43. Bose RK, Hohlbein N, Garcia SJ, Schmidt AM, and van der Zwaag S. *Polymer* 2015;69:228-232.

44. Stukalin EB, Cai L-H, Kumar NA, Leibler L, and Rubinstein M. *Macromolecules* 2013;46(18):7525-7541.

45. Wool RP and O'Connor KM. *Journal of Applied Physics* 1981;52(10):5953-5963.